

RESPONSE OF A MAGLEV VEHICLE MOVING ON A TWO-SPAN FLEXIBLE GUIDEWAY

J. D. Yau*

*Department of Architecture
Tamkang University
Taipei, Taiwan 10620, R.O.C.*

ABSTRACT

This paper is intended to present a preliminary framework for dynamic interaction analysis of a maglev (magnetically levitated) vehicle running on a two-span guideway using a comprehensive iterative approach. A maglev vehicle with electrodynamic suspension (EDS) system is simplified as a two degrees-of-freedom (2-DOF) maglev oscillator tuned by a PID (Proportional-Integral-Derivative) controller. The guideway is modeled as a two-span continuous beam with uniform section. Two sets of equations of motion are written, with the first set for the guideway and the second set for the maglev oscillator traveling on the guideway through a motion-dependent magnetic force. To achieve the stable levitation gap for a maglev vehicle moving on a flexible guideway, Ziegler-Nicholas (Z-N) tuning rules are used to determine the tuning parameters of the PID controller. Numerical simulations demonstrate that the levitation gap affects the dynamic response of the maglev vehicle while little influence on the guideway response since the inertial force of the moving maglev vehicle is much lower than its static load.

Keywords : Free vibration, Guideway, Maglev vehicle, Moving loads.

1. INTRODUCTION

With the advance of modern maglev technology, magnetic forces can lift, propel, and guide a vehicle along an elevated guideway. According to the suspension modes to guide a maglev vehicle moving on guideways, two kinds of maglev technologies have been developed: (1) electromagnetic suspension (EMS, see Fig. 1(a)) with attractive mode; (2) electrodynamic suspension (EDS, see Fig. 1(b)) with repulsive mode [1-3]. The EMS system can lift a vehicle up using attractive forces by the magnets beneath a guide-rail. The EDS system suspends a vehicle above its guide-rail using magnetic repulsive forces to take the train off the U-shaped guideway. To suspend a maglev vehicle at a stable levitation gap (air gap) between the on-board levitation magnets and the guideway, a controllable electromagnetic field is generated in its maglev suspension system. Obviously, the response analysis of a maglev train moving on a flexible guideway is related to not only the dynamics of vehicle/guideway interaction but also the control of maglev system.

Considering the response characteristics of different maglev vehicle models traveling over a flexible guideway, Cai and his co-workers [4,5] concluded that a concentrated-load vehicle model might result in larger responses on the guideway deflections and vehicle accelerations than a distributed-load vehicle model. In the literature review works conducted by Cai and Chen [6], various aspects of the dynamic characteristics, magnetic suspension systems, vehicle stability, suspen-

sion control laws for maglev/guideway coupling systems were discussed. Zheng *et al.* [7,8] investigated the vibration behavior of a maglev vehicle running on a flexible guideway and observed the phenomena of divergence, flutter, and collision on the dynamic stability of a maglev-vehicle traveling on a flexible guideway. However, to the author's knowledge, relatively little research information so far is available on the study of nonlinear vibration control for a maglev vehicle running on a flexible guideway with various speeds [21,22].

In this study, the guideway is modeled as a two-span continuous beam with simply supported ends. A simplified model of a 1D and 2-DOF maglev oscillator tuned by a PID (Proportional-Integral-Derivative) controller [9,10] is employed to simulate the maglev vehicle with EDS system moving on a guideway (see Fig. 2). To resolve the dynamic problem for a two-span guideway under the passage of a running maglev oscillator, the dynamic response of the maglev-oscillator/guideway system is solved by Galerkin's method and then computed using a rigorous iterative approach with Newmark finite difference scheme [11]. Numerical simulations indicate that the maximum acceleration response of a maglev oscillator traveling over a concrete guideway is related to the levitation gap and moving speeds; while the dynamic effects of inertia and levitation gap of the maglev oscillator are little influence on the guideway response in that the vertical inertial force induced by the vibrating oscillator is much lower than the static weight of the oscillator.

* Associate Professor, corresponding author

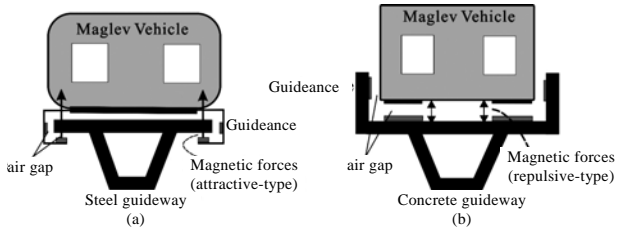


Fig. 1 Schematic diagram of two maglev vehicle systems: (a) Electromagnetic suspension (EMS); (b) Electrodynamic suspension (EDS)

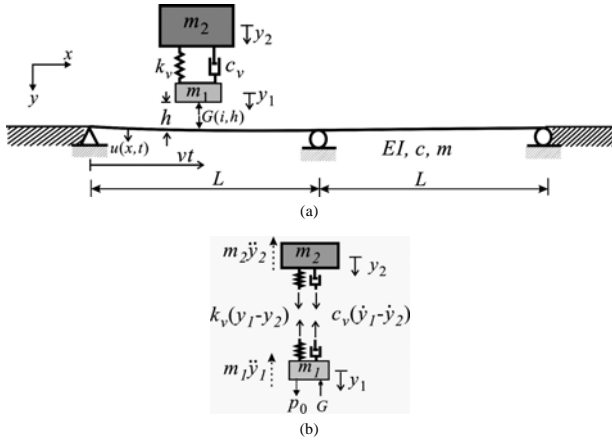


Fig. 2 A schematic diagram of maglev oscillator moving on a two-span guideway (a) maglev oscillator/guideway model; (b) free body diagram of the oscillator

2. THEORETICAL FORMULATION

As shown in Fig. 2, a maglev vehicle with EDS system is levitated by the repulsive force. Since the magnetic force induced by the EDS system is generally not large enough to lift up a maglev vehicle above the guideway at slow speeds, the vehicle must be wheeled to support the vehicle's weight until it reaches a certain liftoff speed (about 100km/h). According to the review work for maglev vehicle systems shown in reference [6], the EMS design system approximates a uniform suspension along the full vehicle length to achieve levitation, whereas the EDS design is closer to discrete loads on the guideway. For this reason, the magnetic force between the vehicle and the guideway is treated as a concentrated force in this study. In order to demonstrate the analytical formulation of vehicle-guideway system tuned by a maglev suspension system, only vertical motions of the dynamic model are considered. The following are the assumptions adopted for the maglev vehicle-guideway system:

- (1) The guideway is modeled as a linear elastic Bernoulli-Euler beam with uniform cross section [12];
- (2) Based on the suspension feature of EDS system with discrete magnetic bogie-sets, a maglev vehicle is modeled as a one dimensional (1D) and 2-DOF maglev oscillator consisting of two concentrated masses, with the top one representing the

mass lumped from the car body and the bottom one the mass of magnetic wheel-set;

- (3) The track surface of the guide-way is assumed to be smooth;
- (4) To keep running safety, the magnetic wheel-set of a maglev vehicle should not contact with the guided rail so that the allowable levitation gap (h) always remains larger than zero, *i.e.*, $h > 0$;
- (5) The dynamic effects including both Coriolis force and centrifugal force induced by the moving oscillator on a deflected beam will be neglected in this study because of the small mass ratio (maglev oscillator to beam) investigated in this study.
- (6) The time delay between the input voltage and the output current of a maglev system is negligible.

2.1 Governing Equations of Motion

As shown in Fig. 2, a maglev oscillator is traveling on a two-span guideway at a constant speed v . The vehicle model is composed of a lumped mass (carriage) supported by a spring-dashpot system connected with a magnetic wheel-set, from which a controllable electromagnetic force is generated to lift the vehicle up at a stable levitation gap (h). Here, we shall use the following symbols to denote the properties depicted in Fig. 1: m = mass of the guideway girder, c = damping coefficient, EI = flexural rigidity, m_1 = lumped mass of magnetic wheel-set, m_2 = lumped mass of car body, c_v = secondary damping coefficient, and k_v = secondary stiffness coefficient. The equation of motion for a simple beam carrying a moving oscillator is given by [13,21,23]

$$m\ddot{u} + c\dot{u} + EIu'''' = G(i, h) \delta(x - vt), \quad (1)$$

with the following boundary conditions:

$$u(0, t) = u(L, t) = u(2L, t) = 0, \quad (2)$$

$$EIu''(0, t) = EIu''(2L, t) = 0, \quad (3)$$

where $(\bullet)' = \partial(\bullet)/\partial x$, $(\bullet)\dot{=} \partial(\bullet)/\partial t$, $u(x, t)$ = vertical deflection of the beam, $\delta(\bullet)$ = Dirac's delta function, y_1 = vertical displacement of the lumped mass m_1 (magnetic wheel-set), and y_2 = vertical displacement of the lumped mass m_2 (carriage). From the equilibrium of free body diagram shown in Fig. 2(b), the equations of motion for the 2-DOF maglev oscillator are written by

$$\begin{bmatrix} m_1 & 0 \\ 0 & m_2 \end{bmatrix} \begin{Bmatrix} \ddot{y}_1 \\ \ddot{y}_2 \end{Bmatrix} + \begin{bmatrix} c_v & -c_v \\ -c_v & c_v \end{bmatrix} \begin{Bmatrix} \dot{y}_1 \\ \dot{y}_2 \end{Bmatrix} + \begin{bmatrix} k_v & -k_v \\ -k_v & k_v \end{bmatrix} \begin{Bmatrix} y_1 \\ y_2 \end{Bmatrix} = \begin{Bmatrix} p_0 - G(i, h) \\ 0 \end{Bmatrix} \quad (4)$$

Here, p_0 = lumped weight of the entire maglev oscillator = $(m_1 + m_2)g$, g = gravity acceleration, $G(i, h)$ denotes the controlled interaction force between the magnetic wheel-set and the guideway (see Fig. 1), which is given by [2,3]

$$G(i, h) = K_0 \left(\frac{i(t)}{h(x, t)} \right)^2, \quad (5)$$

where $K_0 = \mu_0 N_0^2 A_0 / 4 =$ coupling factor [1-3], $\mu_0 =$ vacuum permeability, $N_0 =$ number of turns of the magnet windings, $A_0 =$ pole face area, $i(t) = i_0 + \iota(t) =$ control current, $\iota(t) =$ deviation of control current, $h(x, t) = h_0 + y_1(t) - u(x, t) =$ levitation gap, and $(i_0, h_0) =$ desired values of control current and levitation gap around a specified nominal operating point for a maglev oscillator.

2.2 Equation of Control for Maglev Suspension System

From the expression of the magnetic force $G(i, h)$ in Eq. (5), the motion-dependent nature of the repulsive force plays a key role in resolving the dynamic interaction problem of a maglev oscillator running on a guideway. By adding the two equations from Eq. (4) together, the magnetic force can be expressed in terms of the inertial forces of the maglev oscillator as: $G(i, h) = p_0 - m_1 \ddot{y}_1 - m_2 \ddot{y}_2$. Considering the static equilibrium condition, *i.e.*, $\ddot{y}_1 = \ddot{y}_2 = 0$, for the suspended maglev oscillator in Eq. (5), one can obtain the following relation [7,8,21]

$$G(i_0, h_0) = K_0 (i_0 / h_0)^2 = (m_1 + m_2) g = p_0, \quad (6)$$

where the coupling factor K_0 is equal to $p_0(h_0/i_0)^2$. By the theory of electromagnetic circuits, the electromagnetic equation for magnet current and control voltage in the magnetic suspension system is given by [1-3,21]

$$\Gamma_0 \frac{d(i/h)}{dt} + R_0 i = V, \quad (7)$$

where $\Gamma_0 = 2K_0 =$ initial inductance of the coil winding the suspension magnet, $R_0 =$ coil resistance of electronic circuit, and $V =$ control voltage. Let us adopt the variable transformation as $\gamma = i/h$, Eq. (7) can be rewritten as

$$\Gamma_0 \dot{\gamma} + R_0 h(t) \gamma = V, \quad (8)$$

By introducing the control error function $e = i_0/h_0 - i/h = \gamma_0 - \gamma$ for the parameter γ in a closed-loop control, the control voltage of V can be expressed using PID tuning algorithm as [9,10]

$$V = K_p e + K_i \int_0^t e dt + K_d \dot{e} \quad (9)$$

where $K_p =$ proportional gain, $K_i =$ integral gain, and $K_d =$ derivative gain. Then substituting Eq. (9) into Eq. (8) and differentiating this equation with respect to time, after some mathematical manipulation, one can achieve the following differential equation for control error

$$(K_d + \Gamma_0) \ddot{e} + K_p \dot{e} + K_i e - R_0 \dot{y}_1 \gamma_0 = -R_0 \left[\gamma_0 \frac{\partial u(x, t)}{\partial t} + \frac{\partial(he)}{\partial t} \right]. \quad (10)$$

Here, the nonlinear term of $-R_0 \times d(he)/dt$ has been regarded as a pseudo excitation and moved to the right side of the differential equation [16]. Combining Eqs. (4) and (10) yields the following matrix equation of motion for the maglev oscillator

$$[m_v] \{\ddot{u}_v\} + [c_v] \{\dot{u}_v\} + [k_v] \{u_v\} = \{f_v\}, \quad (11)$$

where $\{u_v\} = \langle y_1 \ y_2 \ e \rangle^T$, and

$$[m_v] = \begin{bmatrix} m_1 & 0 & 0 \\ 0 & m_2 & 0 \\ 0 & 0 & K_d + \Gamma_0 \end{bmatrix}, \quad (12)$$

$$[c_v] = \begin{bmatrix} c_v & -c_v & 0 \\ -c_v & c_v & 0 \\ -R_0 \gamma_0 & 0 & K_p \end{bmatrix}, \quad (13)$$

$$[k_v] = \begin{bmatrix} k_v & -k_v & -2p_0/\gamma_0 \\ -k_v & k_v & 0 \\ 0 & 0 & K_i \end{bmatrix}, \quad (14)$$

$$\{f_v\} = \begin{Bmatrix} -p_0(e/\gamma_0)^2 \\ 0 \\ -R_0 \left[\gamma_0 \frac{\partial u(x, t)}{\partial t} + \frac{\partial(he)}{\partial t} \right] \end{Bmatrix}. \quad (15)$$

To solve the nonlinear dynamic coupling equations shown in Eqs. (1) and (11) for a maglev oscillator running on a two-span guideway, an incremental-iterative procedure will be presented in Section 4.

3. FREE VIBRATION ANALYSIS

According to the work presented by Ayre *et al.* [12], the natural frequency (ω_n) for the n -th mode $\phi_n(x)$ of a two-span continuous beam with equal span can be respectively given as follows:

(1) For odd-numbered modes ($n = 1, 3, 5, \dots$)

$$\omega_n = (n\pi/L)^2 \sqrt{EI/M}, \quad (16)$$

$$\phi_n(x) = \sin \frac{n\pi x}{L}. \quad (17)$$

(2) For even-numbered modes ($n = 2, 4, 6, \dots$)

$$\omega_n = (\lambda_n \pi/L)^2 \sqrt{EI/M}, \quad (18)$$

$$\phi_n(x) = \begin{cases} \sin(\lambda_n \pi x/L) - \kappa_n \sinh(\lambda_n \pi x/L) & 0 \leq x \leq L \\ \sin \frac{\lambda_n \pi(2L-x)}{L} - \kappa_n \sinh \frac{\lambda_n \pi(2L-x)}{L} & L \leq x \leq 2L \end{cases}, \quad (19)$$

$$\kappa_n = \frac{\sin(\lambda_n \pi)}{\sinh(\lambda_n \pi)} = \frac{\cos(\lambda_n \pi)}{\cosh(\lambda_n \pi)}. \quad (20)$$

subject to the characteristic equation: $\tan(\lambda_n \pi) - \tanh(\lambda_n \pi) = 0$. With the free vibration frequencies and modal shapes given in Eqs. (16), (18) and (19), the dynamic response of a two-span beam can be solved using Galerkin's method in the following section.

4. DYNAMIC RESPONSE OF THE TWO-SPAN GUIDEWAY

The solution of dynamic deflection $u(x, t)$ in Eq. (1) can be carried out by Galerkin's method [14-18]. First, multiplying both sides of Eq. (1) with respect to the variation of the dynamic deflection (δu), and then integrating the equation over the beam length L , one can obtain the following virtual work equation:

$$\begin{aligned} & \int_0^{2L} (m\ddot{u} + c\dot{u} + EIU''') \delta u dx \\ &= \int_0^{2L} G(i, h) \delta(x - vt) \delta u dx \\ &= \int_0^{2L} (p_0 - m_1 \ddot{y}_1 - m_2 \ddot{y}_2) \delta(x - vt) \delta u dx, \end{aligned} \quad (21)$$

According to the homogeneous boundary conditions shown in Eqs. (2) and (3), the dynamic deflection can be expressed in terms of the modal functions in Eqs. (17) and (19) as follows [5]:

$$u(x, t) = \sum_{n=1}^{\infty} q_{jn}(t) \phi_n(x); \quad j=1, 2, \quad (22)$$

where $q_{jn}(t)$ means the generalized coordinate associated with the n -th assumed mode of the j -th span of the two-span beam. With the aids of orthogonal property of natural modes given in Section 3, the substitution of Eq. (22) into Eq. (1) yields the following equation of motion for the n -th generalized system [5]:

$$\begin{aligned} m\ddot{q}_{jn} + c\dot{q}_{jn} + k_n q_{jn} &= p_n(t), \\ p_n(t) &= [p_0 - (m_1 \ddot{y}_1 + m_2 \ddot{y}_2)] \psi_n(v, t), \end{aligned} \quad (23)$$

where $k_n = m\omega_n^2$ = generalized stiffness, and the generalized force function is given by

$$\psi_n(v, t) = \begin{cases} \frac{\phi_n(vt)}{L} & n = 1, 3, 5, \dots, \\ \frac{\phi_n(vt)}{L(1 - \kappa_n^2)} & n = 2, 4, 6, \dots, \end{cases} \quad (24)$$

5. SOLUTION PROCEDURE BY THE ITERATIVE METHOD

As the coupling equations of motion shown in Eqs. (11) and (23), the dynamic analysis of a maglev oscillator moving on a guideway is related to not only the dynamic interaction of maglev oscillator-guideway

system but also the magnetic control of the maglev system. Since the control equation in Eq. (10) for maglev suspension system is a nonlinear differential equation in terms of levitation gap (h) and control current (i), this study will propose an iterative method to deal with the dynamic interactions of the maglev oscillator-guideway system.

5.1 Equivalent Stiffness Equations

For the present purpose, let us consider the n -th generalized system of the two-span beam for the formulation of equivalent stiffness equation of maglev oscillator-guideway system. The n -th generalized equation in Eq. (23) associated with the equations of motion for the maglev oscillator in Eq. (11) can be rewritten as follows:

$$\begin{cases} m\ddot{q}_{jn} + c\dot{q}_{jn} + k_n q_{jn} = p_{n,t}, & j=1, 2 \\ [m_v]\{\ddot{u}_v\} + [c_v]\{\dot{u}_v\} + [k_v]\{u_v\} = \{f_v\}, \end{cases} \quad (25)$$

To perform a time-history response analysis for a nonlinear dynamic system, the equations of motion in Eq. (25) are first discretized by Newmark method [11], and then the n th equivalent stiffness equation associated with the vehicle equation for the incremental step from time t to $t + \Delta t$ is expressed as [21]:

$$\begin{cases} K_{n,eq} \times \Delta q_{jn,t+\Delta t} = \Delta p_{n,t+\Delta t}, \\ [K_{v,eq}]\{\Delta u_{v,t+\Delta t}\} = \{\Delta f_{v,t+\Delta t}\}, \end{cases} \quad (26)$$

where the equivalent stiffness terms of ($K_{n,eq}$, $[K_{v,eq}]$) and the load increments of ($\Delta p_{n,t+\Delta t}$, $\{\Delta f_{v,t+\Delta t}\}$) are respectively given as follows

$$\begin{cases} K_{n,eq} = a_0 m + a_1 c + k_n, \\ [K_{v,eq}] = a_0 [m_v] + a_1 [c_v] + [k_v], \end{cases} \quad (27)$$

$$\begin{aligned} \Delta p_{n,t+\Delta t} &= p_{n,t+\Delta t} - R_{n,t}, \\ R_{n,t} &= k_n q_{jn,t} - m(a_2 \dot{q}_{jn,t} + a_3 \ddot{q}_{jn,t}) \\ &\quad - c(a_4 \dot{q}_{jn,t} + a_5 \ddot{q}_{jn,t}), \end{aligned} \quad (28)$$

$$\begin{aligned} \{\Delta f_{v,t+\Delta t}\} &= \{f_{v,t+\Delta t}\} - \{r_{v,t}\}, \\ \{r_{v,t}\} &= [k_v]\{u_{v,t}\} - [c_v](a_4 \{\dot{u}_{v,t}\} + a_5 \{\ddot{u}_{v,t}\}) \\ &\quad - [m_v](a_2 \{\dot{u}_{v,t}\} + a_3 \{\ddot{u}_{v,t}\}). \end{aligned} \quad (29)$$

As shown in Eqs. (26) ~ (29), the symbols are denoted as follows: ($\Delta q_{jn,t+\Delta t}$, $\{\Delta u_{v,t+\Delta t}\}$) = displacement increments generated at the incremental step, and ($R_{n,t}$, $\{r_{v,t}\}$) = effective resistant forces. In respect to the dynamic responses of ($q_{jn,t+\Delta t}$, $\dot{q}_{jn,t+\Delta t}$, $\ddot{q}_{jn,t+\Delta t}$) for the n -th generalized coordinate and ($\{u_{v,t+\Delta t}\}$, $\{\dot{u}_{v,t+\Delta t}\}$, $\{\ddot{u}_{v,t+\Delta t}\}$) for the maglev oscillator at time $t + \Delta t$, they are respectively expressed as [11]

$$\begin{aligned} q_{jn,t+\Delta t} &= q_{jn,t} + \Delta q_{jn}, \\ \dot{q}_{jn,t+\Delta t} &= \dot{q}_{jn,t} + a_6 \ddot{q}_{jn,t} + a_7 \ddot{q}_{jn,t+\Delta t}, \\ \ddot{q}_{jn,t+\Delta t} &= a_0 \Delta q_{jn} - a_2 \dot{q}_{jn,t} - a_3 \ddot{q}_{jn,t}, \end{aligned} \quad (30)$$

$$\begin{cases} \{u_{v,t+\Delta t}\} = \{u_{v,t}\} + \{\Delta u_v\}, \\ \{\dot{u}_{v,t+\Delta t}\} = \{\dot{u}_{v,t}\} + a_6 \{\ddot{u}_{v,t}\} + a_7 \{\ddot{u}_{v,t+\Delta t}\}, \\ \{\ddot{u}_{v,t+\Delta t}\} = a_0 \{\Delta u_v\} - a_2 \{\dot{u}_{v,t}\} - a_3 \{\ddot{u}_{v,t}\}, \end{cases} \quad (31)$$

with the following Newmark coefficients [11]

$$\begin{cases} a_0 = \frac{1}{\beta \cdot \Delta t^2}, \quad a_1 = \frac{\gamma}{\beta \cdot \Delta t}, \quad a_2 = \frac{1}{\beta \cdot \Delta t}, \\ a_3 = \frac{1}{2\beta} - 1, \quad a_4 = \frac{\gamma}{\beta} - 1, \quad a_5 = \frac{\Delta t}{2} \left(\frac{\gamma}{\beta} - 2 \right), \\ a_6 = (1 - \gamma) \Delta t, \quad a_7 = \gamma \cdot \Delta t. \end{cases} \quad (32)$$

and $\beta = 0.25$ and $\gamma = 0.5$. The foregoing procedure can be modified to include the feature of iteration for removing the unbalanced forces. First, the governing equations for the i th iteration of the incremental step are further modified from Eq. (26) as

$$\begin{cases} K_{n,eq} \times \Delta q_{jn,t+\Delta t}^i = \Delta p_{n,t+\Delta t}^i, \\ [K_{v,eq}] \{\Delta u_{v,t+\Delta t}^i\} = \{\Delta f_{v,t+\Delta t}^i\}, \end{cases} \quad (33)$$

where for the first iteration ($i = 1$), $\Delta p_{n,t+\Delta t}^i \equiv \Delta p_{n,t+\Delta t}$ and $\{\Delta f_{v,t+\Delta t}^i\} \equiv \{\Delta f_{v,t+\Delta t}\}$ represent the load increments at the beginning of the incremental step, respectively, and $(\Delta q_{jn,t+\Delta t}^i, \{\Delta u_{v,t+\Delta t}^i\})$ the displacement increments of the n -th generalized displacement $q_{jn,t+\Delta t}^i$ and the vertical displacement $\{u_{v,t+\Delta t}^i\}$ of the maglev oscillator at the i th iteration from time t to $t + \Delta t$. For the following iterations (with $i \geq 2$)

$$\begin{cases} K_{n,eq} \times \Delta q_{jn,t+\Delta t}^i = \Delta p_{n,t+\Delta t}^{i-1}, \\ [K_{v,eq}] \{\Delta u_{v,t+\Delta t}^i\} = \{\Delta f_{v,t+\Delta t}^{i-1}\}. \end{cases} \quad (34)$$

Here, $(\Delta p_{n,t+\Delta t}^{i-1}, \{\Delta f_{v,t+\Delta t}^{i-1}\})$ are interpreted as the unbalanced forces during the following iterative steps. The unbalanced force $\Delta p_{n,t+\Delta t}^{i-1}$ is equal to the difference between the external force $p_{n,t+\Delta t}^{i-1}$ and the effective internal forces $f_{n,t+\Delta t}^{i-1}$ for the n -th generalized system of the beam at time $t + \Delta t$, *i.e.*,

$$\Delta p_{n,t+\Delta t}^{i-1} = p_{n,t+\Delta t}^{i-1} - f_{n,t+\Delta t}^{i-1}, \quad (35)$$

$$f_{n,t+\Delta t}^{i-1} = \Gamma_{n,t+\Delta t}^{i-1} + R_{n,t+\Delta t}^{i-1}, \quad (36)$$

$$R_{n,t+\Delta t}^{i-1} = \begin{cases} k_n q_{jn,t+\Delta t}^{i-1} - m(a_2 \ddot{q}_{jn,t+\Delta t}^{i-1} + a_3 \ddot{q}_{jn,t+\Delta t}^{i-1}) & \text{for } i = 1 \\ -c(a_4 \dot{q}_{jn,t+\Delta t}^{i-1} + a_5 \ddot{q}_{jn,t+\Delta t}^{i-1}) & \\ k_n q_{jn,t+\Delta t}^{i-1} + m \ddot{q}_{jn,t+\Delta t}^{i-1} + c \dot{q}_{jn,t+\Delta t}^{i-1} & \text{for } i > 1 \end{cases}, \quad (37)$$

and the unbalanced force vector $\{\Delta f_{v,t+\Delta t}^{i-1}\}$ for the maglev oscillator at time $t + \Delta t$ is equal to

$$\{\Delta f_{v,t+\Delta t}^{i-1}\} = \{f_{v,t+\Delta t}^{i-1}\} - \{r_{v,t+\Delta t}^{i-1}\}, \quad (38)$$

$$\{r_{v,t+\Delta t}^{i-1}\} = \begin{cases} [k_v] \{u_{v,t+\Delta t}^{i-1}\} - [m_v] (a_2 \{\dot{u}_{v,t+\Delta t}^{i-1}\} + a_3 \{\ddot{u}_{v,t+\Delta t}^{i-1}\}) & \text{for } i = 1 \\ -[c_v] (a_4 \{\dot{u}_{v,t+\Delta t}^{i-1}\} + a_5 \{\ddot{u}_{v,t+\Delta t}^{i-1}\}) & \\ [k_v] \{u_{v,t+\Delta t}^{i-1}\} + [m_v] \{\ddot{u}_{v,t+\Delta t}^{i-1}\} + [c_v] \{\dot{u}_{v,t+\Delta t}^{i-1}\} & \text{for } i > 1 \end{cases}. \quad (39)$$

The dynamic response of the maglev-vehicle/guide-way system can be computed by solving the equivalent stiffness equations shown in Eq. (34), procedures for incremental-iterative dynamic analysis, which involves three major phases: Predictor, corrector and equilibrium-checking [19,21], are outlined in the following section.

5.2 Procedure of Iterations

To compute the dynamic response of the maglev oscillator-guideway system tuned by a PID controller, an incremental-iterative procedure based on modified Newton-Raphson algorithm is summarized as follows:

- (1) Transform the governing differential equation in Eqs. (1) and (11) into a set of generalized equations as Eq. (25);
- (2) Discretize the generalized equations of motion for the dynamic interaction system into a set of equivalent stiffness equations using Newmark finite difference formulas (see Eq. 33). And then perform the following iterative procedure involving three phases: Predictor, corrector and equilibrium-checking.
- (3) Predictor phase

The predictor is concerned with solution of the structural response increments of $(\Delta q_{jn,t+\Delta t}^i, \{\Delta u_{v,t+\Delta t}^i\})$ for given loadings $(\Delta p_{n,t+\Delta t}^{i-1}, \{\Delta f_{v,t+\Delta t}^{i-1}\})$ from the equivalent structural stiffness equations. For the present case, Eq. (33) is used as the predictor subject to the following initial conditions for the 1st iterative step (*i.e.*, for $i = 1$) of each incremental step [16]:

$$q_{n,t+\Delta t}^0 = q_{n,t}^\ell, \quad \dot{q}_{n,t+\Delta t}^0 = \dot{q}_{n,t}^\ell, \quad \ddot{q}_{n,t+\Delta t}^0 = \ddot{q}_{n,t}^\ell, \quad (40)$$

$$f_{n,t+\Delta t}^0 = R_{n,t+\Delta t}^0 + \Gamma_{n,t+\Delta t}^0 = R_{n,t}^\ell + \Gamma_{n,t}^\ell, \quad (41)$$

and

$$\begin{cases} \{u_{v,t+\Delta t}^0\} = \{u_{v,t}^\ell\}, \quad \{\ddot{u}_{v,t+\Delta t}^0\} = \{\ddot{u}_{v,t}^\ell\}, \\ \{\dot{u}_{v,t+\Delta t}^0\} = \{\dot{u}_{v,t}^\ell\}, \quad \{r_{v,t+\Delta t}^0\} = \{r_{v,t}^\ell\}, \end{cases} \quad (42)$$

where ℓ means the last iteration of the previous incremental step at time t .

- (4) Corrector phase

The corrector phase relates to recovery of the internal resistant forces $(f_{n,t+\Delta t}^{i-1}, \{r_{v,t+\Delta t}^{i-1}\})$ from the displacement increments of $(\Delta q_{jn,t+\Delta t}^i, \{\Delta u_{v,t+\Delta t}^i\})$ and the total responses of $(q_{jn,t+\Delta t}^i, \dot{q}_{jn,t+\Delta t}^i, \ddot{q}_{jn,t+\Delta t}^i)$ and $(\{u_{v,t+\Delta t}^i\}, \{\dot{u}_{v,t+\Delta t}^i\}, \{\ddot{u}_{v,t+\Delta t}^i\})$ made available in the predictor. In this phase, the inertial force of $(m_1 \ddot{y}_1 + m_2 \ddot{y}_2)$ in Eq. (23) for the maglev vehicle is updated in an iterative way. Once the resulting force term of $R_{n,t+\Delta t}^{i-1}$ is determined for each iteration, the effective internal forces $(f_{n,t+\Delta t}^{i-1}, \{r_{v,t+\Delta t}^{i-1}\})$ can be computed from Eqs. (36) and (39), and the unbalanced forces $(\Delta p_{n,t+\Delta t}^{i-1}, \{\Delta f_{v,t+\Delta t}^{i-1}\})$ from Eqs. (35) and (38).

(5) Equilibrium-checking phase

In the equilibrium-checking phase, the effective internal forces ($f_{n,t+\Delta t}^{i-1}, \{r_{v,t+\Delta t}^{i-1}\}$) computed from the corrector phase is compared with the external loads ($p_{n,t+\Delta t}^{i-1}, \{f_{v,t+\Delta t}^{i-1}\}$) in Eqs. (36) and (39), the difference being regarded as the unbalanced forces ($\Delta p_{n,t+\Delta t}^{i-1}, \{\Delta f_{v,t+\Delta t}^{i-1}\}$).

(6) Check the unbalanced forces to reach preset tolerances. Whenever the unbalanced forces are greater than preset tolerances,

$$\beta_{tol} = \left[\sum_{k=1\dots} (\Delta f_{v,t+\Delta t}^{i-1})^2 + \sum_{n=1\dots} (\Delta p_{n,t+\Delta t}^{i-1})^2 \right]^{1/2}, \quad (43)$$

say 10^{-3} , another iteration involving the three phases in the steps of (3) ~ (5) is performed.

(7) Repeat the steps (3) ~ (6) for other time instants.

6. NUMERICAL EXAMPLES

As shown in Fig. 2, a maglev oscillator is crossing a two-span guideway at a constant speed v . For the purpose of reducing the influence of a vibrating guideway on ride quality of a running maglev vehicle over it, a concrete girder is used for the two-span guideway [19]. With the same initial control voltage $R_0 i_0$ for the maglev suspension system, the properties of the guideway and maglev oscillator are listed in Tables 1 and 2, respectively. For the purpose of demonstration, only two small desired levitation gaps, *i.e.*, $h_0 = 0.01\text{m}$ and 0.02m , are considered in Table 2. They are named MG-1 and MG-2, respectively. It was well known that if the acceleration response, rather than the displacement response, of a structure is of concern, the contribution of higher modes has to be included in the computation [14-18]. For the vibration simulation of a two-span continuous beam with simply supported ends, the first 12 modes of the shape functions and the time step of 0.001s are employed to compute the acceleration response of the vibrating two-span beam. On the other hand, the acceleration response of a moving vehicle is also used to evaluate the ride quality and running safety of a train traveling over a railway/guideway [20]. In the following numerical examples, the PID tuning parameters are first determined using Ziegler-Nicholas (Z-N) tuning rules and then the dynamic responses of the maglev oscillator and the guideway are computed.

6.1 Application of Z-N Tuning Rules

Z-N tuning rules [9,10] have been proved very useful to determine the parameters of a PID controller in process control system, from which the PID parameters have been given by $K_p = 0.6K_{cr}$, $K_i = 1.2K_{cr}/T_{cr}$, and $K_d = K_{cr}T_{cr}/8$. Here K_{cr} means the critical proportional gain of the PID controller by increasing only the proportional control action (*i.e.*, $K_i = K_d = 0$) K_p from 0 to a critical value K_{cr} so that the output first exhibits an oscillation behavior with a critical period T_{cr} [10]. For the purpose of illustration, let the maglev oscillator cross the two-span guideway at a constant speed of

Table 1 Properties and natural frequencies of the guideway

L (m)	EI (N-m ²)	m (kg/m)	c (N-s/m/m)	T_1^* (s)	T_2 (s)
35	1.33×10^7	3.5×10^3	2.75×10^3	0.40	0.26

* T_n denotes the n -th natural period of the guideway

Table 2 Properties of maglev oscillators

Type	p_0 (N)	m_1 (kg)	m_2 (kg)	c_v (N-s/m)	k_v (N/m)	i_0 (A)	R_0 (Ω)	h_0 (m)	K_0 (m ² -H)
MG-1	8.82×10^4	10^3	8×10^3	2.0×10^4	8.5×10^4	25	1.0	0.01	0.014
MG-2	8.82×10^4	10^3	8×10^3	2.0×10^4	8.5×10^4	25	1.0	0.02	0.056

150km/h. By trials for different values of the proportional gain K_p subject to $h > 0$, the time history responses of the control error function e with the critical parameter K_{cr} to oscillate have been plotted in Fig. 3. It shows that the critical period of the PID controller is almost independent upon the initial levitation gap h_0 and a larger proportional gain can help mitigate the response amplitude of the controller. Meanwhile, the transient responses of vertical acceleration of the lumped masses of m_1 and m_2 for the moving maglev oscillator have been depicted in Figs. 4 and 5, respectively. The simulation results indicate that a smaller desired levitation gap (*i.e.*, MG-1) may lead to smaller vibration amplitude for the maglev oscillator since a larger proportional gain K_{cr} is required to restrict the fluctuation gap to vibrate in a small region around the chosen nominal operating point for a 2DOF sprung mass unit. However, the acceleration amplitudes of the MG-2 (with larger desired air gap but smaller tuning parameter of K_{cr}) in Figs. 4 and 5 are significantly larger than those of the MG-1 (with smaller desired air gap but larger K_{cr}). It means that if both the maximum acceleration amplitudes of the MG-1 and MG-2 are limited to a specific level, the tuning gains of the MG-2 should be increased. Even so, from the practical view point of maglev transport operation, as the dynamic response of a maglev vehicle can satisfy the stringent requirement of acceleration response ($< 0.05g$) for the assessment of riding comfort and running safety of a maglev vehicle, the controller with smaller tuning gains has still achieved its control performance for the maglev system.

On the other hand, Fig. 6 depicts the time history responses of mid-point acceleration for the departure span of the continuous guideway traversed by the running vehicles of MG-1 and MG-2, respectively. The numerical results illustrate that the dynamic effects of inertia and levitation gap of a moving maglev oscillator are small on the concrete guideway response since the magnetic force acting on the guideway is approximate to $G(i, h) = p_0 - (m_1 \ddot{y}_1 + m_2 \ddot{y}_2) \approx p_0$, in which both the vertical accelerations of \ddot{y}_1 and \ddot{y}_2 are smaller than $0.05g$. This conclusion is consistent with that presented in Ref. [5,6].

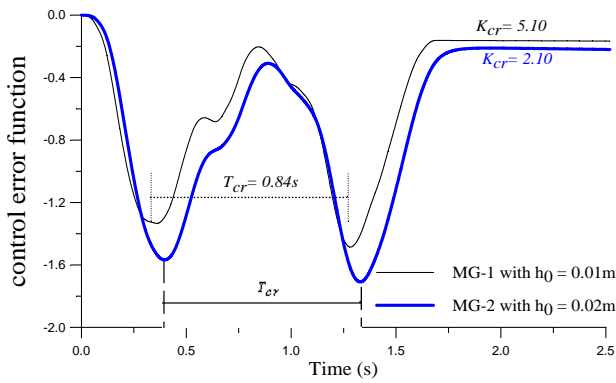


Fig. 3 Transient oscillation with a critical period T_{cr}

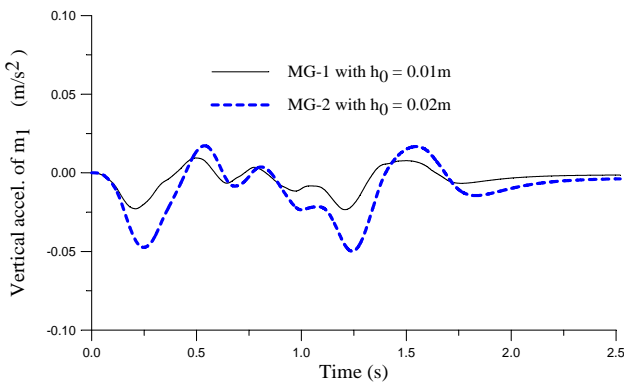


Fig. 4 Time history of vertical acceleration response for maglev wheel-set

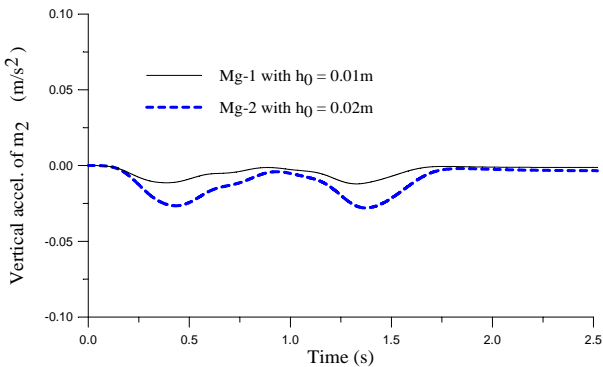


Fig. 5 Time history of vertical acceleration response for maglev oscillator

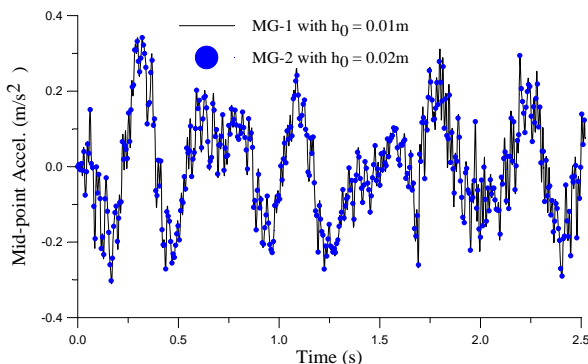


Fig. 6 Midpoint acceleration of the departure span

6.2 Determination of PID Tuning Parameters

As described in Section 2, a maglev vehicle with EDS system is levitated by the repulsive force as it reaches a liftoff speed (about 100km/h). Thus let us range the moving speeds of the maglev oscillator from 100km/h to 450km/h. By trials for different values of K_p under the condition: levitation gap $h > 0$ mentioned in example 6.1, Fig. 7 shows the relations of $K_{cr} - T_{cr}$ against various speeds for the MG-1 ($h_0 = 0.01\text{m}$) and the MG-2 ($h_0 = 0.02\text{m}$), respectively. It indicates that the present maglev oscillator possessing smaller levitation gap requires more proportional gains to achieve the requirement of allowable levitation gap for a maglev system to oscillate.

From the $K_{cr} - T_{cr}$ relation depicted in Fig. 7, there exists a minimum value for critical proportional gains at $T_{cr} = 0.4\text{s}$ associated with the critical speed $v_{cr} = 315\text{km/h}$ ($= 87.5\text{m/s}$), which coincides with the fundamental period ($T_1 = 0.4\text{s} = L/v_{cr}$) of the two-span beam. It means that the control error function e of the PID controller can oscillate with the guideway response in a synchronous way. For the purpose of demonstration, let us suppose the proportional parameter K_p in Eq. (10) as a damping coefficient in the dynamic equation of electromagnetic control. Thus the phenomenon of oscillation for a dynamic system with smaller damping will not be damped out swiftly. Figure 8 shows the corresponding maximum vertical acceleration of the maglev oscillator against speeds. This figure indicates that the maglev suspension system with larger critical proportional parameters will offer more control gains and result in smaller response for the moving maglev oscillator.

6.3 Maximum Response Analysis

Considering the PID parameters proposed by Z-N tuning rules ($K_p = 0.6K_{cr}$, $K_i = 1.2K_{cr}/T_{cr}$, and $K_d = K_{cr}T_{cr}/8$) in Example 6.2, the maximum vertical accelerations of the lumped mass m_2 (carriage) of the MG-1 and MG-2 have been plotted in Fig. 9 against speeds. The simulation results indicate that the smaller desired

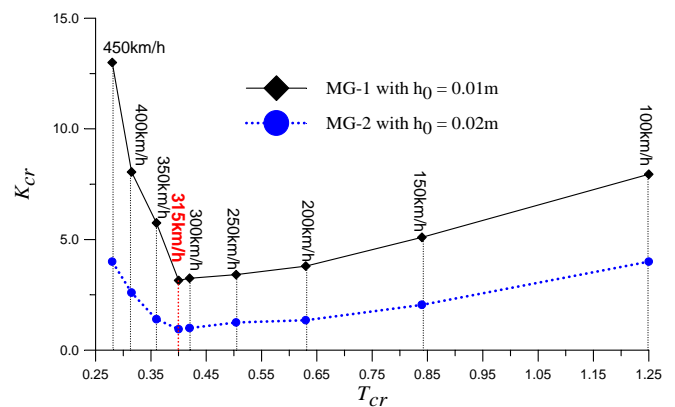


Fig. 7 Relation of $K_{cr} - T_{cr}$ against various speeds

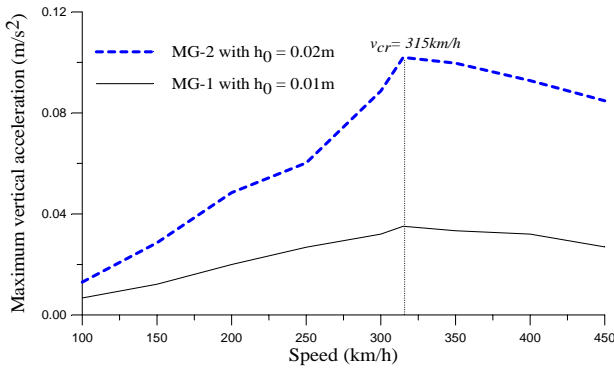


Fig. 8 Maximum vertical acceleration of the maglev oscillator with critical K_{cr}

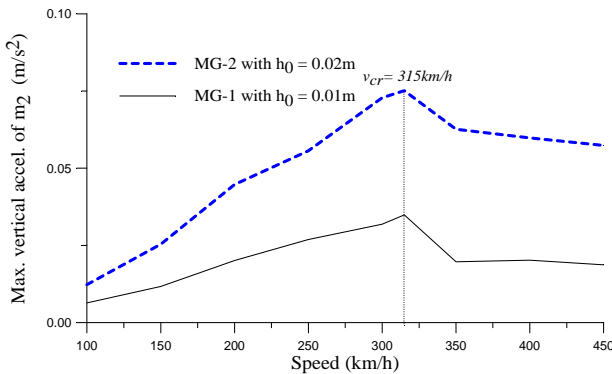


Fig. 9 Maximum vertical acceleration of maglev oscillator with Z-N tuning parameters

levitation gap may lead to smaller acceleration response for a maglev oscillator since it requires more tuning gains to control its levitation gap not to contact with guided rail. In addition, the maximum acceleration reaches its peak value at the critical speed $v_{cr} = 315\text{km/h}$. As described in example 6.2, the PID tuning gains (K_p , K_b , K_d) obtained from the corresponding critical proportional gain K_{cr} reach their minimum values at the critical speed v_{cr} . Thus the acceleration amplitude of the maglev oscillator moving at this speed is amplified significantly. From the practical point of maglev transport operation, as the dynamic response of a maglev vehicle can satisfy the stringent requirement of acceleration response ($< 0.05\text{g}$) for the assessment of riding comfort and running safety of a maglev vehicle, the PID controller with minimum tuning gains has achieved its optimum control performance for the maglev suspension system.

On the other hand, Fig. 10 plotted the maximum acceleration along the guideway subject to the maglev oscillator moving with four speeds (100, 200, 300, and 400km/h), respectively. This figure indicates that the acceleration amplitude of the guideway increases along with the increase of moving speeds and the dynamic response of the departure span is larger than that of the arrival span. Moreover, the responses associated with other higher modes are also excited due to some secondary peaks on the acceleration response curves [7,13-15].

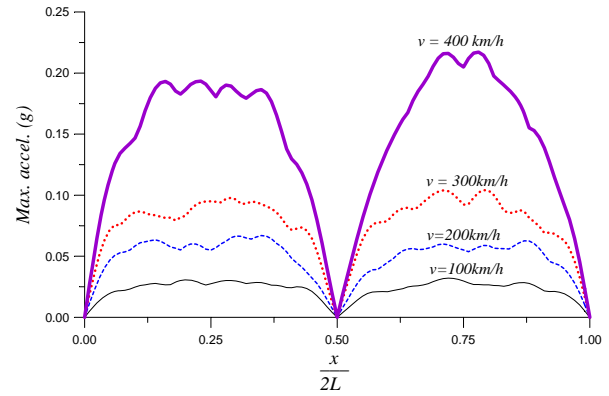


Fig. 10 Maximum acceleration along the guideway against various speeds

7. CONCLUDING REMARKS

This paper presents a rigorous iterative approach to deal with the dynamic problem of a 1D and 2DOF maglev oscillator within a stable levitation gap, where a PID tuning algorithm based on Z-N tuning rules is proposed to control the magnetic force. Then, the dynamic response of the maglev oscillator-guideway system can be solved by Galerkin's method and computed using an iterative approach with Newmark's finite difference formulas. From the numerical studies, the following conclusions are reached:

As a maglev vehicle moves on a flexible guideway at the critical speed $v_{cr} (= L/T_1)$, which produces a periodic force acting on the guideway with the fundamental period of the guideway, the tuning gains of the PID controller may reach minimum but the acceleration response of the maglev vehicle is amplified significantly.

Compared with the tuning gains of the MG-1 (the maglev oscillator with smaller air gap), the MG-2 (with larger air gap) requires less PID gains to tune its vibration around the chosen nominal operating point although the acceleration amplitudes of the MG-2 are significantly larger than those of the MG-1. Even so, if the dynamic response of a maglev vehicle can be controlled within the requirement of allowable acceleration limitations ($< 0.05\text{g}$) for ride quality and running safety of a maglev vehicle, the PID controller with smaller tuning gains has still achieved its control performance for the maglev system.

Under the stringent requirement of maximum vehicle's acceleration smaller than 0.05g , the inertial effect of a moving maglev oscillator is little influence on the concrete guideway response in that the vertical inertial force induced by the vibrating oscillator is much lower than the static weight of the oscillator.

Since the present maglev vehicle model is a rather simplified maglev oscillator, a further study to develop a more realistic maglev vehicle on which continuously distributed/discrete magnets are mounted can be continuously conducted for the assessment of dynamic interactions of maglev train/guideway coupling system.

ACKNOWLEDGMENTS

Part of this research is supported by Grant No. NSC 97-2221-E-032-022-MY2, National Scientific Council, Taiwan. The author would like to thank this financial grant. Parts of the theory and illustrative examples presented in this study have been referred to as the paper entitled "Response analysis of a moving maglev sprung mass system," at the Proceedings of the 26th National Conference on Mechanical Engineering, National Cheng-Kung University, Tainan, Taiwan, Nov. 20-21 [24].

REFERENCES

1. Sinha, P. K., *Electromagnetic Suspension, Dynamics and Control*, Peter Peregrinus Ltd., London, U. K. (1987).
2. Bittar, and Moura Sales A. R., "H₂ and H_∞ Control for Maglev Vehicles," *IEEE, Control Systems Magazine*, **18**, pp. 18–25 (1998).
3. Trumper, D. L., Olson, S.M. and Subrahmanyam, P. K., "Linearizing Control of Magnetic Suspension Systems," *IEEE, Transactions on Control Systems Technology*, **5**, pp. 427–438 (1997).
4. Cai, Y. and Chen, S. S., "Numerical Analysis for Dynamic Instability of Electrodynamical Maglev Systems," *Shock and Vibration*, **2**, pp. 339–349 (1995).
5. Cai, Y., Chen, S. S., Rote, D. M. and Coffey, H.T., "Vehicle/Guideway Dynamic Interaction in Maglev Systems," *Journal of Dynamic Systems, Measurement, and Control*, ASME, **118**, pp. 526–530 (1996).
6. Cai, Y. and Chen, S. S., "Dynamic Characteristics of Magnetically-Levitated Vehicle Systems," *Applied Mechanics Reviews*, ASME, **50**, pp. 647–670 (1997).
7. Zheng, X. J., Wu, J. J. and Zhou, Y. H., "Numerical Analyses on Dynamic Control of Five-Degree-Of-Freedom Maglev Vehicle Moving on Flexible Guideways," *Journal of Sound and Vibration*, **235**, pp. 43–61 (2000).
8. Zheng, X. J., Wu, J. J. and Zhou, Y. H., "Effect of Spring Non-Linearity on Dynamic Stability of a Controlled Maglev Vehicle and Its Guideway System," *Journal of Sound and Vibration*, **279**, pp. 201–215 (2005).
9. Astrom, K. J. and Hagglund, T., *Automatic Tuning of PID Controllers*, Instrument Society of America (1988).
10. Ogata, K., *Modern Control Engineering*, 3rd Ed., Prentice-Hall Intl. Inc., N. J. (1997).
11. Newmark, N. M., "A Method of Computation for Structural Dynamics," *Journal of the Engineering Mechanics Division*, ASCE, **85**, pp. 67–94 (1959).
12. Ayre, R. S., Ford, G. and Jacobsen, L. S., "Transverse Vibration of a Two-Span Beam Under Action of a Moving Constant Force," *Journal of Applied Mathematics*, **17**, pp. 1–12 (1950).
13. Yang, Y. B., Yau, J. D. and Wu, Y. S., *Vehicle-Bridge Interaction Dynamics*, World Scientific, Singapore (2004).
14. Yau, J. D., "Vibration of Arch Bridges Due to Moving Loads and Vertical Ground Motions," *Journal of the Chinese Institute of Engineers*, **29**, pp. 1017–1027 (2006).
15. Yau, J. D. and Fryba, L., "Response of Suspended Beams Due to Moving Loads and Vertical Seismic Ground Excitations," *The Journal of Structural Engineering*, **29**, pp. 3255–3262 (2007).
16. Yau, J. D. and Yang, Y. B., "Vibration of a Suspension Bridge Installed with a Water Pipeline and Subjected to Moving Trains," *The Journal of Structural Engineering*, **30**, pp. 632–642 (2008).
17. Yau, J. D., "Vibration of Parabolic Tied-Arch Beams Due to Moving Loads," *International Journal of Structural Stability and Dynamics*, **6**, pp. 193–214 (2006).
18. Yau, J. D., "Train-Induced Vibration Control of Simple Beams Using String-Type Tuned Mass Dampers," *Journal of Mechanics*, **23**, pp. 329–340 (2007).
19. Bohn, G. and Steinmetz, G., "The Electromagnetic Levitation and Guidance Technology of the Transrapid Test Facility Emsland," *IEEE, Transactions on Magnetics*, **20**, pp. 1666–1671 (1984).
20. Fan, Y. T. and Wu, W. F., "Dynamic Analysis and Ride Quality Evaluation of Railway Vehicles—Numerical Simulation and Field Test Verification," *Journal of Mechanics*, **22**, pp. 1–11 (2006).
21. Yau, J. D., "Vibration Control of Maglev Vehicles Traveling Over a Flexible Guideway," *Journal of Sound and Vibration*, **321**, pp. 184–200 (2009).
22. Yau, J. D., "Response of a Maglev Vehicle Moving on a Series of Guideways with Differential Settlement," *Journal of Sound and Vibration*, **324**, pp. 816–831 (2009).
23. Lin, H. P., "Dynamic Responses of Beams with a Flexible Support Under a Constant Speed Moving Load," *Journal of Mechanics*, **24**, pp. 195–204 (2008).
24. Yau, J. D., "Response Analysis of a Moving Maglev Sprung Mass System," *Proceedings of the 26th National Conference on Mechanical Engineering*, National Cheng-Kung University, Tainan, Taiwan, Nov. 20-21 (2009).

(Manuscript received June 2, 2008, accepted for publication June 25, 2009.)